Homochiral Conglomerates and Racemic Crystals in Two Dimensions: Tartaric Acid on Cu(110)

Sara Romer, Bahar Behzadi, Roman Fasel, and Karl-Heinz Ernst*[a]

Abstract: Two-dimensional lattice structures formed by racemic tartaric acid on a single crystalline Cu(110) surface have been studied and compared with the enantiopure lattices. At low coverage, the doubly deprotonated bitartrate species is separated into two-dimensional conglomerates showing opposite enantiomorphism. At higher coverage, however, a singly deprotonated monotartrate species forms a heterochiral, racemic crystal lattice. While the enantioseparated bitartrate system undergoes decomposition at the same temperature as the enantiopure system, the racemic monotartrate lattice has a lower thermal stability than the enantiopure lattice of identical periodicity and surface density. At monolayer saturation coverage, the pure enantiomers form a denser lattice than the racemate. This is in contrast to the three-dimensional tartaric acid crystals, where the racemate crystallizes in a lattice of higher density, which is also more thermally stable than the enantiopure tartaric acid crystals.

Keywords: chirality · crystal growth · surface chemistry

Introduction

Chiral molecules crystallize from racemic solutions either into homochiral conglomerates or into racemic crystals containing equal numbers of left- and right-handed molecules.[1,2] In his historic experiment, Pasteur made use of the fact that chiral molecules can form enantiomorphs, that is, crystals showing macroscopic chirality.[3] However, the mechanism of the transfer of chirality from single molecules to the resulting enantiomorphous crystals is poorly understood.[4] This is actually part of the general problem that macroscopic crystal shapes are still not predictable from the molecular structures.[5] In particular the solvent or impurities influence the shape of a macroscopic crystal to a large extent. Studying well-defined 2D chiral model systems on surfaces without such influences, therefore, can help to get more insight into the transfer of chirality from single molecules into larger ensembles.[6] Although the vast majority of chiral molecules crystallize as non-separated racemates, it has been predicted that two-dimensional enantioseparation on a surface should occur more easily than in three-dimensional crystals.[7] Due to confinement in the plane certain symmetry elements, for example, center of inversion or the glide plane parallel to the surface, are precluded and enhanced chiral interactions are expected.[7b,8] Indeed, only a few examples of racemic 2D crystals are known[9] and most experimental studies confirmed the scenario of spontaneous lateral resolution of chiral molecules into homochiral two-dimensional crystallites, observed as two-dimensional enantiomorphism.[8,10] It is noteworthy that, due to symmetry breaking upon adsorption, achiral molecules can also form two-dimensional chiral motifs on the surface.[11]

Herein we report the observation that a single racemic compound forms, depending on the coverage on the surface, either homochiral domains ("2D conglomerates") or racemic (heterochiral) 2D crystals. For this study we chose the "classic" tartaric acid (TA) adsorbed on a copper(110) surface. The adsorption of enantiopure (2*R*,3*R*)-TA on this surface has previously been studied in great detail.[12] The studies showed that at room temperature TA is adsorbed as a monotartrate with only one carboxylate group interacting with the surface (Figure 1a). After thermal activation, however, the second carboxylate group also interacts with the substrate, that is, annealing to 405 K leads to the formation of bitartrate species (Figure 1b).[13] In its sawhorse-like adsorbate geometry, the bitartrate molecule is distorted into a zigzag conformation, as predicted by theoretical studies[14] and experimentally confirmed by our group.[15] With increas-

---

[a] Dr. S. Romer, B. Behzadi, Dr. R. Fasel, Dr. K.-H. Ernst
Nanoscale Materials Science
Swiss Federal Institute for Materials Science and Technology (EMPA)
Überlandstrasse 129, 8600 Dübendorf (Switzerland)
Fax: (+41) 1-823-4034
E-mail: karl-heinz.ernst@empa.ch

DOI: 10.1002/chem.200400962

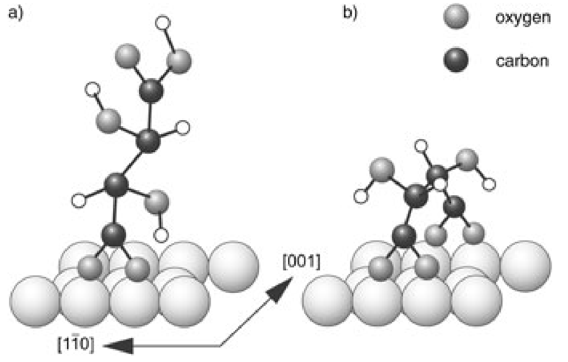

Figure 1. Molecular species formed by adsorption of tartaric acid on Cu(110) at 405 K: a) singly deprotonated monotartrate at saturation coverage; b) doubly deprotonated bitartrate at low coverage.

ing coverage, a rearrangement into monotartrate occurs, since this allows a higher adsorbate density.[16] In both species, each carboxylate directly interacts with two copper atoms of the close-packed row along the [1 $\bar{1}$ 0] direction. At these temperatures, the dissociated carboxyl hydrogen atoms are not stable on the surface and desorb as molecular hydrogen. Several ordered surface phases have been observed for the (2*R*,3*R*)-enantiomer at 405 K: a (9 0, 1 2) bitartrate phase, a (4 0, 2 1) phase, and a (4 1, 2 5) phase at saturation.[12] The adsorbate lattice periodicities are specified in Equation (1) with respect to the substrate lattice by the transformation matrix (m_{11} m_{12}, m_{21} m_{22}), which links the adsorbate lattice vectors (b_1, b_2) to the substrate lattice vectors (a_1, a_2):[17]

$$\begin{pmatrix} b_1 \\ b_2 \end{pmatrix} = \begin{pmatrix} m_{11} & m_{12} \\ m_{21} & m_{22} \end{pmatrix} \begin{pmatrix} a_1 \\ a_2 \end{pmatrix} \qquad (1)$$

The (9 0, 1 2) and the (4 1, 2 5) lattices are 2D enantiomorphous, that is, they lack mirror symmetry. The (2*S*,3*S*)-enantiomer forms the respective mirror lattices, that is, (9 0, −1 2) and (−4 1, −2 5), if reflection with respect to the [001] substrate direction is considered. The (4 0, 2 1) lattices of the two enantiomers, however, are undistinguishable, since this lattice expresses no enantiomorphism in low energy electron diffraction (LEED). Herein we describe the ordered adsorbate lattices formed by *racemic* TA on Cu(110) at 405 K and discuss the results with respect to the findings for the enantiopure TA system.

Results and Discussion

Figure 2 shows the two LEED patterns observed after exposure of the Cu(110) surface, held at 405 K, to racemic TA. A (9 0, ±1 2) lattice forms at lower coverage (Figure 2, left), while at saturation coverage a (4 0, 2 1) lattice is observed (Figure 2, right). Overall, both lattices possess the C_{2v} mirror symmetry of the substrate. However, the (9 0, ±1 2) lattice must be explained as a superposition of the two enantiomorphous bitartrate lattices of the pure enantiomers.[18] Therefore, we conclude that this LEED pattern reflects a lattice structure in which the enantiomers are laterally separated into homochiral (9 0, 1 2)-(*R*,*R*)-TA and (9 0, −1 2)-(*S*,*S*)-TA domains on the surface. The primary electron beam probes an area that contains both enantiomorphous homochiral lattices. The size of the homochiral domains can roughly be estimated from the LEED pattern by taking the instrumental resolution, the so-called transfer width, into account. The fact that for an electron energy of 20 eV sharp superstructure diffraction spots are observed, indicates that the domains must have a diameter of more than 20 nm on average.[19] In principle, this LEED pattern might be also explained by the formation of diasteriomeric pairs, which form the two mirror domains by chance. Due to an oblige angle of the adsorbate mesh with respect to the substrate lattice, two equal alignments are possible which can be interconverted only by the mirror operation. However, this scenario was found to be very unlikely in theoretical studies performed on this system. Adsorption of the (*S*,*S*)-enantiomer into the (*R*,*R*)-(9 0, 1 2) adsorbate grid is 10 kJ mol^{-1} higher in energy than the homochiral arrangement.[14]

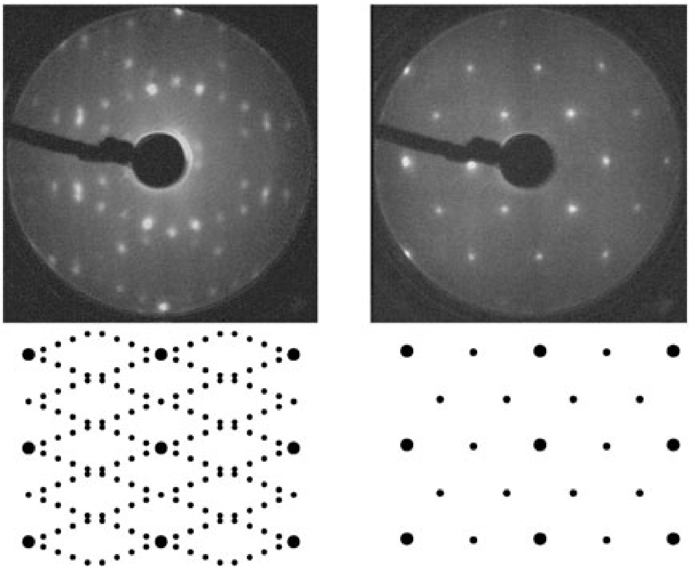

Figure 2. LEED patterns observed after adsorption of racemic tartaric acid on Cu(110) at 405 K. Left: At low coverage a superposition of (9 0, 1 2) and (9 0, −1 2) patterns is observed ($E_P = 20$ eV). This (9 0, ±1 2) pattern is explained by lateral separation of the enantiomers into homochiral, enantiomorphous conglomerates. Right: At saturation coverage a (4 0, 2 1) lattice is observed ($E_P = 38$ eV).

As already mentioned, the (4 0, 2 1) lattice has been observed for the pure enantiomers as well.[12] This is particularly noteworthy since in three dimensions no case is known thus far in which a chiral molecule crystallizes in an achiral crystal lattice. In this 2D monotartrate lattice the lateral interactions must be substantially lower than for the bitartrate, and the outcome of the long-range structure is governed by the substrate geometry rather than the molecular configuration. The identical (4 0, 2 1) lattices for racemate and pure enantiomers do not allow a conclusion on lateral separation in the racemic monotartrate layer. However, the fact that for racemic TA the (4 0, 2 1) mesh is the monolayer saturation structure, while for the pure enantiomers another structure is established at higher coverage, is a strong indication for a racemic (4 0, 2 1) lattice. For homochiral monotartrate crystallites, we would expect, in analogy to bitartrate, the observation of a conglomerate (±4 1, ±2 5) lattice upon further adsorption.

Table 1. Comparison of molecular density and thermodynamic stability of TA racemate and enantiomers for the crystalline bulk and the monolayer lattices. The 3D values for the melting points (m.p.) and the molecular volumes (V_{mol}) were taken from the literature, while the values for the 3D sublimation enthalpy (ΔH_{sub}), the saturation coverage (θ_{max}), and the activation energy (ΔE_{dec}) as well as the pre-exponential factor (k) for thermally induced decomposition on the surface are from this work.

	3D			2D		
	m.p. [°C]	ΔH_{sub} [kJ mol^{-1}]	V_{mol} [Å^3]	k [s^{-1}]	ΔE_{dec} [kJmol^{-1}]	θ_{max} $10^{14}\times$cm^{-2}
racemate	205[27]	138	139[28]	10^{14}	142	2.5
enantiomer	170[27]	129	142[29]	10^{15}	162	2.78

In order to evaluate the difference in saturation coverages, we compared the signal intensities of the C1s XPS (X-ray photoelectron spectroscopy) peaks and of temperature programmed desorption (TPD) curves for racemate and the pure enantiomers. Figure 3 shows the respective exposure/coverage (θ) functions. The theoretical coverages of the three lattice structures are indicated as dashed lines. For the (9 0, ±1 2) and the (4 0, 2 1) lattices, $^1/_6$ and $^1/_4$ molecules per Cu surface atom have been proposed, respectively.[12] Normalization between both experimental methods has been performed for the values at saturation. For the absolute coverage calibration, the XPS signal area obtained for the racemic (4 0, 2 1) lattice has been assigned to a value of $\theta = 0.25$ (see structure model discussion further below). Because racemic TA has a higher heat of sublimation (Table 1), and all compounds were sublimed at the same temperature, the racemic TA flux per time was lower, which explains the smaller coverage increase for the racemate (Figure 3). The linear rise until saturation indicates that the neutral TA molecule can—physisorbed in a precursor adsorbate state—migrate laterally over the surface until free surface sites are found. Consequently, the number of free substrate sites has no influence on the adsorption kinetics and the sticking coefficient is expected to be close to unity up to saturation.

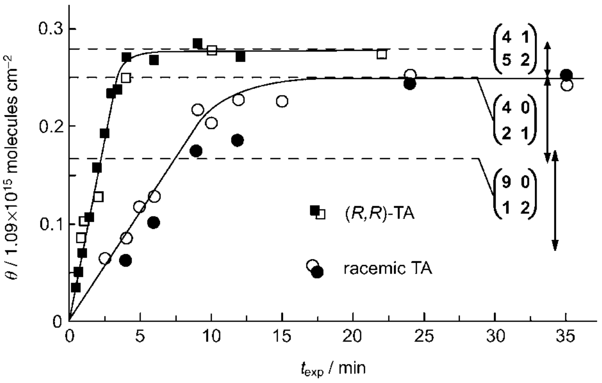

Figure 3. Comparison of the coverage/exposure relation for pure (2*R*,3*R*)-TA (squares) and racemic TA (circles). The data points represent the signal areas obtained from TPD (CO_2 evolution, filled symbols) and XPS (C1s, open symbols) experiments. The data from both methods were normalized to each other on the average of the values at saturation. Coverage calibration was done by assigning the normalized C1s XPS intensity from the (4 0, 2 1)-racemic lattice at saturation to the coverage of 0.25 molecules per Cu surface atom. The theoretical coverages for the lattice structures (dashed lines) and the coverage regimes for which these are observable in LEED (arrows) are indicated. Lines to guide the eye are based on the XPS data.

Interestingly, the saturation coverage for the (*R*,*R*)-enantiomer lies slightly above the saturation coverage for the racemate, just outside the estimated error margin of the XPS method (±5%). In order to understand why a higher coverage is achieved for the pure enantiomers, we briefly discuss lattice structures for enantiopure monotartrate. Figure 4 presents tentative structure models for the (4 0, 2 1) and the (4 1, 2 5) lattice, respectively. The unit cells are indicated.[20] For the (4 0, 2 1) grid one molecule per unit cell, that is, one molecule per four Cu surface atoms ($\theta = 0.25$), is the only reasonable coverage value for a monotartrate species bound to two copper atoms. For the enantiomorphous (4 1, 2 5) lattice, on the other hand, either five or six molecules per unit cell are possible, with coverages of 0.278 ($\theta = ^5/_{18}$) and 0.33 ($\theta = ^6/_{18}$), respectively.[21] Our XPS and TPD results show saturation below $\theta = 0.3$ and thus clearly favor a lattice with five molecules per unit cell. The (4 1, 2 5) structure model shown in Figure 4 takes the formation of monotartrate dimers into account, as observed by infrared spectroscopy.[12] The alternation of monotartrate dimers and monomers along the b_1 adsorbate lattice direction is a chiral motif and has previously been suggested for this lattice as well as for an enantiomorphous (4 0, 2 3) monotartrate lattice generated at room temperature.[12] The arrangement of the monomers between the monomer/dimer chains shown in Figure 4 is one of few reasonable choices, which are not further discussed here. This lattice model rationalizes why coverages higher than $\theta = 0.25$ are achieved for the enantiopure layer, but not observed for the racemic mixture. An additional TA molecule can only be adsorbed on the site between four monotartrate molecules in the (4 0, 2 1) lattice if it has the same handedness. This shows that the racemic (4 0, 2 1) lattice layer is not separated into homochiral domains, because no further molecule can be added. Therefore, the formation of the enantiopure (4 1, 2 5) lattice can be considered as a process in which chiral recognition takes place! Since formation of homochiral dimers was only found for coverages above $\theta = 0.25$ in the above-mentioned infrared studies, and for the racemate no lattice structure with $\theta > 0.25$ is observed here, we conclude that the chiral recognition is based on the impossibility of heterochiral dimer formation close to monolayer saturation.

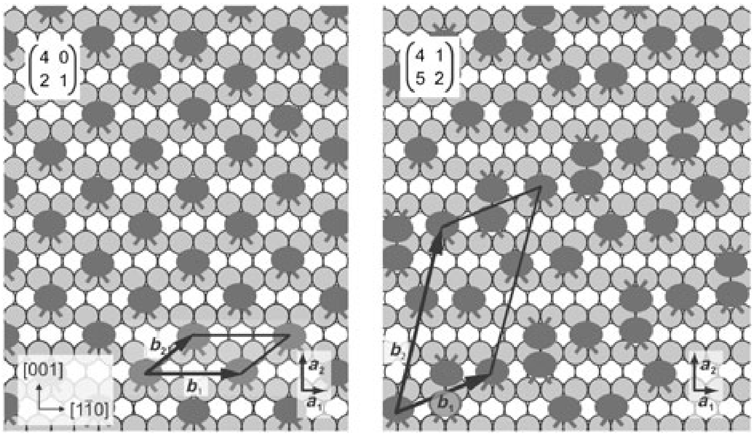

Figure 4. Tentative structure models for the (4 0, 2 1) lattice (left) and the (*R*,*R*)-(4 1, 2 5) lattice (right). The absolute coverages are five molecules per 20 substrate atoms and per 18 Cu substrate atoms, respectively. For the (4 1, 2 5) lattice, the formation of monotartrate dimers, alternating with monotartrate monomers along the [221] direction, is proposed.

The strongest support for the scenario of enantiomeric separation in case of bitartrate, but a racemic lattice for the high coverage monotartrate comes from the thermal stability of the respective enantiopure and racemic lattice structures. On Cu(110), TA undergoes decomposition into stable gas phase products such as CO_2, H_2O and H_2 after the thermal decomposition reaction. We also observed residual carbon on the surface via XPS. With the exception of carbon monoxide, which we assign as fragment of CO_2 generated in the mass spectrometer, no other products have been detected. Consequently, the following surface decomposition reaction for mono- and bitartrate is proposed:

$$\text{OOC-HCOH-HCOH-COO}\mathbf{H} \rightarrow 2\,CO_2 + 2\,H_2O + 2\,C + {}^{1}\!/_{2}\mathbf{H_2}$$

Figure 5 shows the TPD spectra for carbon dioxide (44 amu) formed by this reaction after adsorption of (*R*,*R*)- and racemic TA at 405 K. With increasing coverage, a strong peak shift to higher temperatures is observed. For the low coverage bitartrate lattices, however, no differences between racemate and pure enantiomers are observed.[22] Close to saturation, the desorption peaks become extremely narrow. This phenomenon is known for certain decomposition reactions of carboxylic acids on metallic surfaces.[23] In order to see this behavior, the molecular species must be stabilized above the thermal stability of the single molecule on the surface. Therefore, this effect is observed for close-packed adsorbate systems, not allowing upper parts of the molecule to further interact easily with the substrate. The decomposition follows autocatalytic kinetics, because free surface sites serving as catalyst for the reaction are, in turn, generated upon decomposition. Hence, the reaction rate depends on the coverage (θ) and on the number of free surface sites $1-\theta$ [Eq. (2)]:

$$\frac{d\theta}{dt} = A\,\theta\,(1-\theta)\,e^{-E/RT} \qquad (2)$$

Once the decomposition reaction in the close-packed lattice starts, the newly created free surface sites cause an exponential increase in turnover rate. Because the TA decomposition temperature is higher than the desorption temperature of the gas-phase-stable reaction products, these products desorb instantaneously and cause a relatively large increase in pressure above the surface in a small temperature interval. This led to the expression "surface explosion" for this type of surface reaction.[23]

The decomposition temperature of the racemic (4 0, 2 1) lattice is about 8 K lower than of the enantiopure (4 0, 2 1) lattice (Figure 5). We explain this difference by a chiral ensemble effect:[22] The reaction rate depends not exclusively on the number of molecules and on the number of free surface sites, but is also influenced by the molecular structure of adjacent molecules. Because coverage and periodicity are identical in both (4 0, 2 1) lattices, the difference in thermal stability between pure enantiomers and racemate must be due to a heterochiral lattice in the racemic layer.

Another difference between racemate and pure enantiomers is observed for the TPD spectra reflecting the transition from the homochiral bitartrate lattices into the enantiopure or the racemic (4 0, 2 1) lattice (grey curves in Figure 5). At coverages just below the narrow "surface explosion" peaks, the respective peak from the racemic layer is much wider than from the enantiopure lattice. Again, this is an indication of higher heterogeneity in this transition regime. We recall that the conversion to monotartrate is induced when additional TA is adsorbed onto the homochiral bitartrate domain.[16] The bitartrate species becomes hydrogenated by the "incoming" tartaric acid molecule. The then released substrate binding site becomes occupied by the TA molecule which served as hydrogen donor and actually induced the conversion reaction. This process is independent of the handedness of the newly adsorbing TA molecule and consequently leads to a racemic lattice upon exposure to a racemic mixture. In order to test this local racemic mixing model, we exposed a (*R*,*R*)-bitartrate (9 0, 1 2) lattice at a coverage of $\theta = {}^{1}\!/_{8}$ to pure (*S*,*S*)-TA. This experiment led to a (4 0, 2 1) lattice with a saturation coverage of $\theta = {}^{1}\!/_{4}$, as determined via XPS. Exposure to more (*S*,*S*)- or (*R*,*R*)-TA

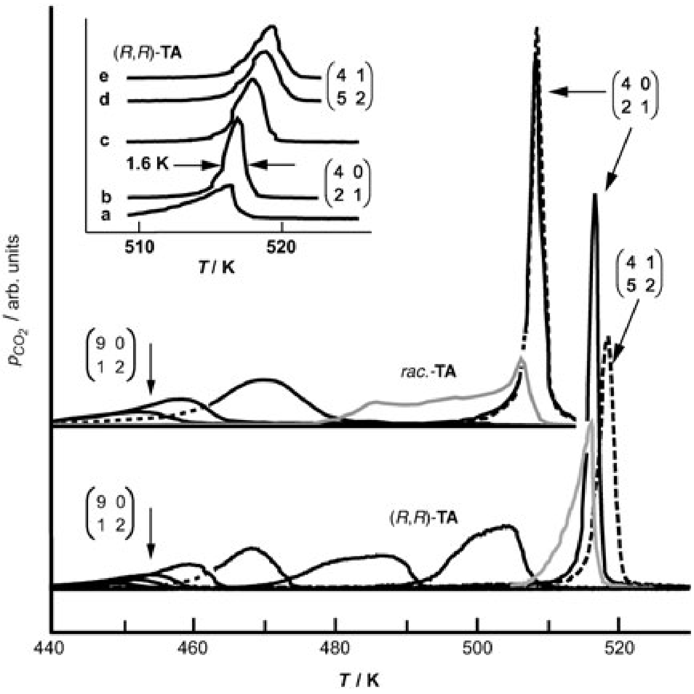

Figure 5. Reaction induced carbon dioxide desorption spectra for racemic TA (top) and (2*R*,3*R*) TA (bottom) with increasing coverage. The peaks for which LEED patterns of best quality have been observed are indicated. The inset illustrates the change in peak shape during the conversion from the (4 0, 2 1) lattice to the (4 1, 2 5) lattice for the pure enantiomers. The desorption peaks at high coverages are very narrow, indicating an autocatalytic decomposition reaction. See text for more details.

did not lead to other lattice structures nor to higher coverages. In addition, the TPD decomposition temperature of this layer was almost identical to the one of the racemic layer.[22] This shows that, no matter whether homochiral domains of opposite chirality or a complete enantiopure bitartrate layer are present at the beginning, the outcome for a racemic monotartrate system is the same: a heterochiral (4 0, 2 1) saturation lattice. For the monotartrate lattices generated at room temperature we observed a similar situation: while for (*R*,*R*)-TA an enantiomorphous (4 0, 2 3) lattice follows a (4 0, 2 1) with increasing coverage,[12] the saturation lattice for the racemate is (4 0, 2 1).

Another detail is shown in the inset of Figure 5. During the transition from the (4 0, 2 1) to the (4 1, 2 5) lattice the decomposition temperature of the pure enantiomers increases by another 3 K. This can be explained by the higher activation barrier for an interaction with the surface at higher surface density. The desorption peak, however, becomes broader with respect to the peak of the (4 0, 2 1) lattice, that is, from 1.6 to 2.2 K full width at half maximum (FWHM). A reasonable explanation is the increased heterogeneity in the lattice due to the coexistence of dimers and monomers on the surface, introducing slightly different decomposition pathways.

Interestingly, the system of achiral succinic acid ($HOOC\text{-}CH_2\text{-}CH_2\text{-}COOH$) on Cu(110) is very similar to racemic TA here. For the bisuccinate species, a (9 0, ±1 1) and a (7 0, ±1 1) lattice have been observed.[24,25] Due to symmetry breaking interactions with the surface, this molecule becomes chiral upon adsorption and forms enantiomorphous domains. Because no chiral preference is given, the global outcome is achiral, that is, both enantiomorphous lattices coexist on the surface and appear as superposition in LEED, just like racemic TA in its bitartrate form. Interestingly, when an additional chiral influence is present, for example, (*R*,*R*)- or (*S*,*S*)-tartrate, the entire monolayer is driven into homochirality.[25] Also identical to the racemic monotartrate here is the (4 0, 2 1) or c(4×2) lattice that is formed by the monosuccinate.

Finally, we discuss different thermodynamical and structural properties of the racemate and pure enantiomers and compare these for the 2D crystals on Cu(110) and the TA bulk (Table 1). Stability and density of the enantiopure lattices, with respect to the racemic systems, are higher for the 2D crystal, but lower in the 3D bulk. The pre-exponential factor and the activation energy of the TA decomposition reaction were determined via systematic heating rate variation.[26] Both, the pre-exponential factor and the activation energy are higher for the pure enantiomer lattices. The homochiral lattice is stabilized by an additional $20\,\mathrm{kJ\,mol^{-1}}$ with respect to the racemic lattice. The stiffer lattice due to stronger lateral binding is also reflected in one order of magnitude increase in the frequency factor. In order to react with the catalytically active substrate sites, an upper part of the molecule must be unhinged from the molecular lattice, and obviously this initial step is influenced by the chirality of the adjacent molecules. Since succinic acid is thermally much more stable than tartaric acid on Cu(110),[24] we further conclude that in the initial step of the thermally induced decomposition the OH groups on the TA molecule is involved.

Conclusions

Depending on the coverage, tartaric acid can either become laterally enantioseparated or form a racemic lattice. In its bitartrate form at lower coverages homochiral enantiomorphous lattice structures are generated, while the monotartrate species present at higher coverage crystallizes into a racemic lattice. Compared with the pure enantiomers, the bitartrate lattices are identical in stability, while the racemic monotartrate lattice has lower stability. Furthermore, a higher lattice density is achieved for the pure enantiomers at saturation coverage. This observation is in contrast to the three-dimensional bulk crystalline tartaric acid, where the racemic lattice is denser and has a higher thermal stability than that of the pure enantiomers.

Experimental Section

The experiments have been carried out in a stainless steel ultra-high vacuum (UHV) chamber ($p = 5\cdot10^{-10}$ mbar) equipped with facilities for temperature programmed desorption (TPD) using a quadrupole mass spectrometer, low energy electron diffraction (LEED), and X-ray photoelectron spectroscopy (XPS). The polished copper(110) single crystal (Matek, Jülich) could be resistively heated to 1000 K and liquid nitrogen cooled to about 85 K. Cleaning of the Cu surface was achieved by prolonged argon ion bombardment in vacuum ($E=600$ eV, $p_{\mathrm{Ar}}=2\cdot10^{-5}$ mbar, $I=4\times10^{-6}$ A cm^{-2}). The sputter-damaged surface was annealed at 1100 K for one minute. After several cycles of this treatment, the surface did not show any impurities in XPS and the LEED pattern consisted of a sharp and bright (1×1) structure with low background intensity. This cleaning procedure was also applied after every TPD experiment.

Tartaric acid (Aldrich 99.95 %) deposition was performed with a home-made Knudsen cell. The Cu crystal was exposed to the collimated molecular beam effusing from the Knudsen cell which was held at 120 °C during sublimation. For the preparation of bitartrate and the (4 0, 2 1) and (4 1, 2 5) monotartrate lattices, the Cu sample was held, if not mentioned otherwise, at 405 K during deposition. Relative coverages have been monitored via XPS by measuring the C1s signal plus normalization to the Cu3s substrate peak. For the absolute coverage calibration, XPS spectra were taken for the LEED structures which have been previously characterized by Ortega Lorenzo et al. by using STM, LEED and FTIR.[12] The sample temperature was measured by a chromel/alumel thermocouple and controlled by a special regulator and ramp generator. The TPD spectra were acquired with a linear heating rate of 4.1 K s^{-1} with the surface normal in line of sight of the mass spectrometer. The heating rate variation experiments, from which activation barriers were determined, have been performed with heating rates from 0.8 to 8.5 K s^{-1}. Angle resolved TPD experiments showed no differences in the intensity distribution of different decomposition products. The heats of sublimation for racemate and the pure (*S*,*S*)-enantiomer were calculated via the Clausius–Clapeyron equation. The sublimation rates with varying temperatures of both substances were determined with a mass spectrometer mounted in line of sight of the Knudsen cell.

Acknowledgements

This work was supported by the Schweizerischer Nationalfonds zur Förderung der Wissenschaften (SNF) and by the Board of the Swiss Federal Institute of Technology (ETH Board). We thank R. Raval, University of Liverpool, B. Kahr, University of Washington, M. Gottfried, Universität Erlangen, and M. Parschau, EMPA Dübendorf, for fruitful discussions. Technical support by T. Rytz is acknowledged.

---

[1] J. Jacques, A. Collet, S. H. Wilen, *Enantiomers, Racemates and Resolutions*, Wiley, New York, **1981**.

[2] C. P. Brock, W. B. Schweitzer, J. D. Dunitz, *J. Am. Chem. Soc.* **1991**, *113*, 9811.

[3] L. Pasteur, *Ann. Chim. Phys.* **1848**, *24*, 442.

[4] L. Addadi, S. Weiner, *Nature* **2001**, *411*, 753.

[5] On the contrary, it is possible to link observed crystal shape to molecular chirality, see: L. Addadi, Z. Berkovitch-Yellin, I. Weissbuch, M. Lahav, L. Leiserowitz, *Top. Stereochem.* **1986**, *16*, 1.

[6] R. Fasel, M. Parschau, K.-H. Ernst, *Angew. Chem.* **2003**, *113*, 5336; *Angew. Chem. Int. Ed.* **2003**, *42*, 5178.

[7] a) M. V. Stewart, E. M. Arnett, *Top. Stereochem.* **1982**, *13*, 195; b) I. Kuzmenko, I. Weissbuch, E. Gurovich, L. Leiserowitz, M. Lahav, *Chirality* **1998**, *10*, 415.

[8] M. Lahav, L. Leiserowitz, *Angew. Chem.* **1999**, *111*, 2691; *Angew. Chem. Int. Ed.* **1999**, *38*, 2533; .

[9] a) I. Weissbuch, M. Berfeld,, W. Bouwman, K. Kjaer, J. Als-Nielsen, M. Lahav, L. Leiserowitz, *J. Am. Chem. Soc.* **1997**, *119*, 933; b) S. De Feyter et al, *Angew. Chem.* **2001**, *113*, 3317; *Angew. Chem. Int. Ed.* **2001**, *40*, 3217; c) K.-H. Ernst, M. Parschau, R. Fasel, *e-J. Surf. Sci. Nanotech.* **2004**, *2*, 136.

[10] a) S. de Feyter, F. C. de Schryver, *Chem. Soc. Rev.* **2003**, *32*, 139 and references therein.

[11] S. M. Barlow, R. Raval, *Surf. Sci. Rep.* **2003**, *50*, 201 and references therein.

[12] M. Ortega Lorenzo, S. Haq, T. Bertrams, P. Murray, R. Raval, C. J. Baddeley, *J. Phys. Chem. B* **1999**, *103*, 10661.

[13] The term "bitartrate" is actually used for the singly deprotonated tartrate ion: $C_4H_5O_6^-$, while the doubly deprotonated ion ($C_4H_4O_6^{2-}$) is termed "tartrate". However, in order to avoid confusion, we use here the "surface science nomenclature" as introduced by Raval in ref. [12].

[14] L. A. M. M. Barbosa, P. Sautet, *J. Am. Chem. Soc.* **2001**, *123*, 6639.

[15] R. Fasel, J. Wider, C. Quitmann, K.-H. Ernst, T. Greber, *Angew. Chem.* **2004**, *116*, 2913; *Angew. Chem. Int. Ed.* **2004**, *43*, 2853.

[16] M. Ortega-Lorenzo, V. Humblot, P. Murray, C. J. Baddeley, S. Haq, R. Raval, *J. Catal.* **2002**, *205*, 123.

[17] a) R. L. Park, H. H. Madden, Jr., *Surf. Sci.* **1968**, *11*, 188; b) ref. [11], Appendix A.

[18] M. Ortega-Lorenzo, C. J. Baddeley, C. Muryn, R. Raval, *Nature* **2000**, *404*, 376.

[19] G. Ertl, J. Küppers, Low energy electrons and surface chemistry, 2nd ed., VCH, Weinheim, **1985**, p. 233.

[20] It has been suggested to use values larger than 90° as appropriate angles between adsorbate grid vectors; see: W. N. Unertl, Physical structure, in: Surface Crystallography (Eds.: S. Holloway, N. V. Richardson), Handbook of Surface Science, *Vol. 1*, Elsevier, Amsterdam, **1996**, Chapter 1. This would lead to other matrix notations for the adlayer mesh than used here. However, for compatibility reasons and in order to avoid confusion, we use the vector arrangement proposed by Raval (ref. [12]), that is, the angle between the superlattice vectors are smaller than 90°.

[21] The suggestion by Raval and co-workers that the (4 1, 2 5) structure has a coverage of 0.3, cannot be reconciled with a true (4 1, 2 5) mesh, since the corresponding number of molecules per unit cell, that is, 5.4, is not an integer.

[22] B. Behzadi, S. Romer, R. Fasel, K.-H. Ernst, *J. Am. Chem. Soc.* **2004**, *126*, 9176.

[23] a) J. L. Falconer, R. J. Madix, *Surf. Sci.* **1974**, *46*, 473; b) J. McCarty, J. L. Falconer, R. J. Madix, *J. Catal.* **1973**, *30*, 235; c) R. J. Madix, J. L. Falconer, A. M. Suszko, *Surf. Sci.* **1976**, *54*, 6.

[24] V. Humblot, M. Ortega Lorenzo, C. J. Baddeley, S. Haq, R. Raval, *J. Am. Chem. Soc.* **2004**, *126*, 6460.

[25] M. Parschau, S. Romer, K.-H. Ernst, *J. Am. Chem. Soc.* **2004**, *126*, 15398.

[26] P. A. Redhead, *Vacuum* **1962**, *12*, 203.

[27] C. A. Bischoff, P. Walden, *Ber. Dtsch. Chem. Ges.* **1889**, *22*, 1819.

[28] A. Gerstacker, *Z. Kristallogr.* **1927**, *66*, 421.

[29] a) Y. Okaya, N. R. Stemple, M. I. Kay, *Acta Crystallogr.* **1966**, *21*, 237; b) H. Hope, U. de la Camp, *Acta Crystallogr. Sect. A* **1972**, *28*, 201.

Received: September 20, 2004
Revised: February 11, 2005